COBEM 2023 27TH INTERNATIONAL CONGRESS OF MECHANICAL ENGINEERING

ABCM Brazilian Society of Mechanical Sciences and Engineering
27th ABCM International Congress of Mechanical Engineering
December 04-08, 2023, Florianópolis-SC, Brazil

COB-2023-0503
INFLUENCE OF ANNEALING ON PLA MECHANICAL AND THERMAL RESISTANCE

Felipe dos Anjos Rodrigues Campos
Lucas Melo Queiroz Barbosa
Kauã Ferreira de Almeida
Pedro Henrique Veiga Oliveira
Gabriel Candido Andrzejewski
Paulo Eduardo Vieira De Sousa Filho
Federal University of Uberlandia, School of Mechanical Engineering, Av. João Naves de Ávila, 2121, Bloco 1M, 38400-902, Uberlândia, MG, Brazil
filipin_anjos@hotmail.com, lmqbarbosa@gmail.com, kaualmeida2013@hotmail.com, pedroh.veiga.o@gmail.com, portinoy-gabriel@hotmail.com, paulofilhopf2@gmail.com

Álisson Rocha Machado
Graduate Program in Mechanical Engineering, Pontifícia Universidade Católica do Paraná – PUC-PR, R. Imaculada Conceição, 1155, Bairro Prado Velho, CEP 80215-901, Curitiba/PR, Brasil
alissonr.machado@gmail.com

Abstract. *Fused Filament Fabrication (FFF) is a widely used additive manufacturing process. It involves extruding a polymer filament through a heated nozzle, which moves in three axes and deposits the material in layers on a flat bed. As the plastic cools and solidifies in each layer, it receives some thermal energy from subsequent depositions. Understanding the thermoplastic properties, particularly the glass transition temperature (when molecules become more mobile and adherent) and the crystallization temperature (when molecules organize into crystals, providing more strength and less ductility), is essential for this process. The objective of this work was to evaluate the impact of annealing on specimens, allowing the materials to crystallize and improve layer contact and adhesion. Tensile and flexural tests were conducted according to ASTM D638 and ASTM D6272 standards to verify changes in mechanical properties, while heat deflection temperature (ASTM D648) tests and geometric deviation measurement evaluated the thermal resistance and warping, respectively. The methodology involved a complete factorial experimental design with 2 levels and 3 factors (2^3), for each of the tests. A universal testing machine was used for both tensile and flexural tests, while the heat deflection tests were conducted in an Arduino automatically controlled electric oven to ensure a steady temperature increase rate of 2 °C per minute. Results have shown small changes in the material resistance due to printing, and little dimensional changes as well, with greater effects from printing parameters, which could happen due to the sensitivity of the material to humidity, since it is contrary to what is expected. However, the thermal resistance of the polymer improved greatly, showing an interesting feature of the annealing process for PLA and its wide range of uses in the industry and consumer end applications within additive manufacturing.*

Keywords *Additive manufacture, Annealing, Impact resistance, Crystallinity*

1. INTRODUCTION

Additive manufacturing (AM) using the Fused Filament Fabrication (FFF) process has demonstrated excellent capabilities for producing parts with complex geometries at lower costs compared to other AM techniques. This process essentially involves an extrusion system with a movable nozzle, which deposits molten material layer by layer. The technique has gained prominence in automotive, biomedical, artistic, and educational applications, primarily attributed to the increased utilization of plastics and polymeric composites across various fields. Predominantly, thermoplastic polymers are employed, known for their high fluidity near their melting temperatures, typically ranging from 180 to 300 °C, while maintaining strong mechanical properties at room temperature.

A common challenge in parts manufactured by Fused Filament Fabrication (FFF) is the reduced strength at the interface between printed layers. This phenomenon can lead to failures under various testing conditions, including tension (Cole et al., 2016; Sood et al., 2010; Fernandez-Vicente et al., 2016), bending (Sun et al., 2008), torsion (Rodríguez et al., 2000), and compression (Percoco et al., 2012), whether the loading is static or impact-related. Particularly in the case of impact loading, the lack of adhesion between layers can facilitate the initiation and propagation of cracks between them (Sharafi et al., 2021). As a result, the interlaminar bond strength of additively manufactured parts remains a significant obstacle in their design and utilization. Figure 1 illustrates this phenomenon, where the insufficient contact between deposited layers impedes the proper interlocking of polymeric chains, which is a critical mechanism for achieving

interfacial adhesion in printed objects (Sun et al., 2008). Addressing this issue is crucial for further enhancing the quality and durability of items manufactured using FFF technology.

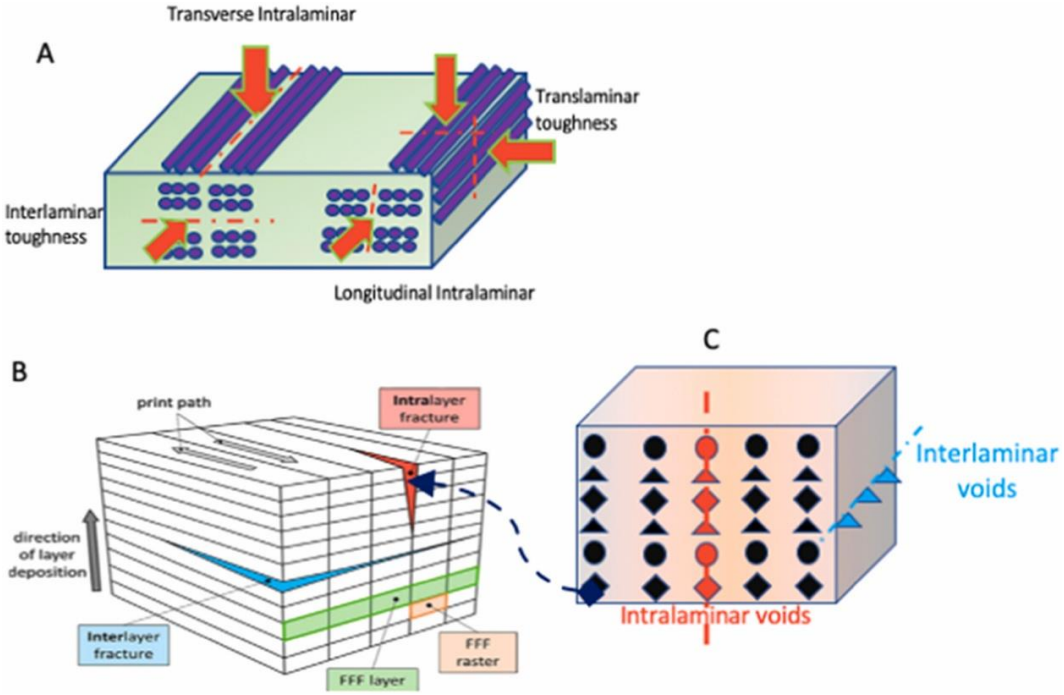

Figure 1. (a) Possible failure modes in parts printed by FFF on composite fiber filaments or (b) purely polymeric filaments with (c) voids between the deposited layers. Adapted from Sharafi et al (2021).

Various methods have been employed to enhance this interlayer adhesion, including the optimization of printing parameters such as scanning speed, printing bed temperature, nozzle temperature, deposition rate, among others (Aliheidari et al., 2017; Johanson, 2016). Additionally, alternative approaches encompass the utilization of adaptive layer height algorithms (Allen and Trask, 2015), the introduction of plasticizers into the filament (Wang et al., 2014), microwave irradiation (Sweeney et al., 2017), or post-processing techniques like annealing (Hart et al., 2018; Bhandari et al., 2019). While these methods have demonstrated improvements in mechanical performance, it is noteworthy that the resultant properties often fall short of achieving the mechanical strength and toughness comparable to materials produced using more traditional methods such as injection molding.

The mechanisms associated with interlayer adhesion between polymers have been described in the context of polymer joining and welding, providing insights into how various variables in additive manufacturing influence the strength of parts produced by Fused Filament Fabrication (FFF). In general, the adhesion process is governed by the molecular diffusion of polymer chains from one layer to another. Therefore, it is highly dependent on factors such as the fluidity and surface tension of the molten polymer, the interface temperature relative to the polymer's glass transition temperature (referred to as Tg, which determines chain mobility), the time and pressure at the layer interface, and phenomena related to possible crystallization in certain polymers. During deposition, the polymer is heated to a temperature (T) higher than its Tg and is then extruded over the previously deposited layer, which in many cases has already cooled below the Tg. This results in rapid and repeated fluctuations of the interface temperature, oscillating above and below the Tg (Sun et al., 2008; Seppala et al., 2017). This heat transfer process is highly sensitive to printing conditions, as they significantly influence the flow and distribution of heat within the part over time (Mackay et al., 2017; Seppala et al., 2017). The complexity of the thermal history thus represents another critical factor in achieving strong adhesion and interlaminar strength.

Another noteworthy aspect is the phenomenon of crystallization. Depending on the molecular structure of the polymer chains, they can organize into a structured and tightly packed configuration. This phenomenon occurs more readily in polymers with shorter, more rigid, unbranched chains and without side groups (Canevarolo Junior, 2006). Since the deformation of polymers relies heavily on the movement and stretching of polymeric chains, properties such as tensile strength, yield strength, modulus of elasticity, and impact behavior strongly depend on the crystallinity content within the material's volume (Matyjaszewski and Möller, 2000). This content varies according to the cooling conditions of the thermoplastic material from its viscous state, as it gradually organizes into its crystalline structure, which has lower free energy (Ebewele, 2000).

Many works focused on improving the resistance of parts produced by FFF have already addressed the effects of parameters that modify the geometry and moment of inertia of the part, such as wall thickness, percentage and type of

infill. In this regard, this work aimed to verify now the influence of annealing and printing parameters that affect thermal history on the mechanical and thermal properties of PLA. The samples were printed by FFF process and evaluated by tensile tests, flexural tests, geometric deviation, and heat deflection test. The discussions made contribute to a better understanding of these phenomena by students, researchers, and hobbyists.

2. METODOLOGY

2.1 Preparetions of the samples

All the samples utilized in this study were fabricated from natural polylactic acid (PLA) filaments with a diameter of 1.75 mm, sourced from the manufacturer 3DFila. Test specimens were produced through additive manufacturing using the Fused Filament Fabrication (FFF) method. A Creality Ender 3 3D printer was employed to create different geometries for each test standard, with variations in printing parameters and annealing, as detailed in Table 1. For each type of test, a complete factorial experimental design was implemented, involving 2 levels and 3 variables (2^3). Sample parameters denoted as A to H were employed for the tensile tests following ASTM D638 (2014), four-point bending flexural tests per ASTM D6272 (2017), and heat deflection temperature assessments based on ASTM D648 (2018). The latter test measures the polymer's resistance to heat under small mechanical stresses. It's important to note that during the printing process, all other parameters were held constant, including layer height (0.2 mm), printing speed (50 mm/s), and nozzle size (0.4 mm).

Table 1. Complete factorial experimental design 2^3.

Test condition	Tbed	Tnozzle	Annealling
A	85	215	without
B	85	200	without
C	50	200	without
D	50	215	without
E	85	215	with
F	85	200	with
G	50	200	with
H	50	215	with

2.2 Annealing and heat deflection tests

To investigate the impact of post-treatment through annealing, the printed components were subjected to controlled heating in an electric oven. Specifically, half of the printed samples in each test underwent annealing using a 10 L electric oven from Britânia, with a power rating of 1050 W. The annealing process involved placing the samples inside the oven before activating it and then heating them for a duration of 20 minutes, within a temperature range approximately between 100°C to 120°C.

The left-side curves in Figure 2 illustrate this process, showing the internal temperature of the oven as measured by four type K thermocouples connected to MAX31855 Arduino-compatible modules. An Arduino Uno microcontroller with an ATmega processor 328 was utilized as a signal acquisition board to record the data on the computer, employing the CoolTerm 2.0 software. Following the completion of the annealing process, the oven was switched off, and the parts were allowed to cool inside for an additional 20 minutes.

On the other hand, the heat deflection tests were conducted by heating the oven in an automatically controlled manner to achieve a constant temperature rise rate of 2°C per minute, as stipulated by the ASTM D648 standard. To accomplish this, the oven's heating element was controlled using an electronic relay connected to an Arduino. This system would switch off the power if the actual temperature exceeded the desired value at any given time and vice versa, effectively creating a closed-loop control system. The heating curve, which demonstrates the precision of the system, is also displayed in Figure 2. It's worth noting that, in contrast to the traditional values recommended by ASTM, a stress of 1.2 MPa was applied to the samples during this test.

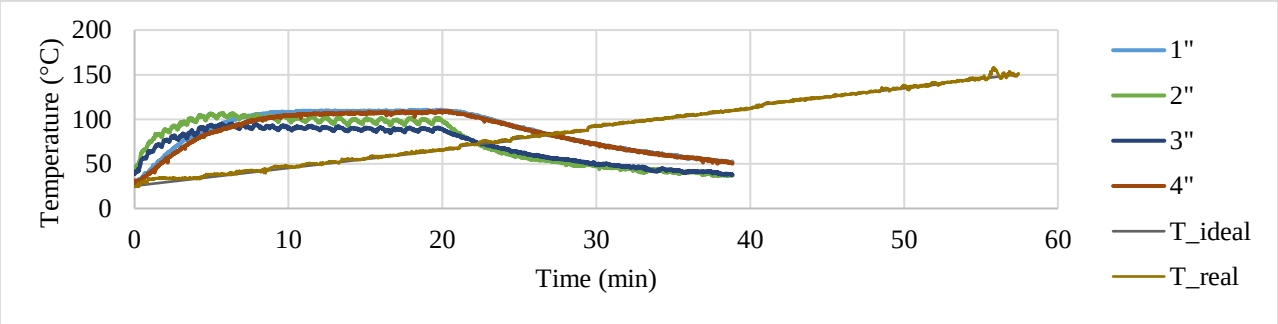

Figure 2. Temperature in the oven measured by thermocouples connected to Arduino, during annealing and during heat deflection tests.

2.3 Tensile and flexural tests

The tensile tests were carried with the type 5 specimen of ASTM D638, shown in Figure 3, where the mains dimensions are L = 9.5 mm, W = 3.2 mm, WO = 9.5 mm, T = 3 mm and LO = 63.5 mm. The flexural tests were carried with rectangular section beams of dimensions 127 mm x 12.7 mm x 3 mm.

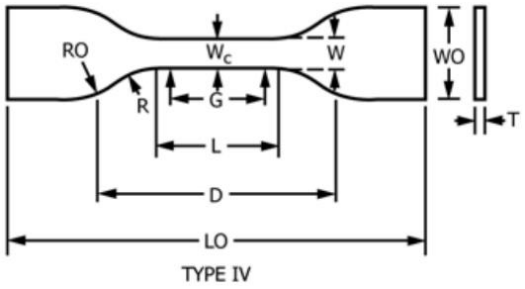

Figure 3. Type 5 test specimen according to ASTM D638 (2014).

Both tests were conducted using a custom-built universal testing machine, which shares similarities with well-established models (referenced in the literature). The testing apparatus was equipped with four load cells arranged in parallel, each having a maximum capacity of 50 kg and a resolution of 0.05 g, with a manufacturer-specified precision of 5 g. The entire setup was connected to an Arduino for data acquisition, employing HX711 modules, following the same approach as explained for the annealing tests. To generate the required tension, an electric DC motor with reduction gear was utilized, generating a torque of 3 kgf·m, resulting in a maximum tensioning force of approximately 150 kg. It's worth noting that, due to equipment limitations, an intermediary shear rate of 0.04 was employed instead of the typical 0.01 or 0.1 values recommended by the standard. During testing, both load and displacement were acquired simultaneously. Subsequently, the results were analyzed using Microsoft Office Excel 2016, with calculations of tension and deformation performed in accordance with the standards. Examples of the curves generated during testing are presented in Figure 4. Displacement measurements were obtained at the machine's axle using an encoder to record the rotation of the primary tensioning screw. Key mechanical properties, including maximum stress, deformation at breaking, and elastic modulus, were calculated for comparison.

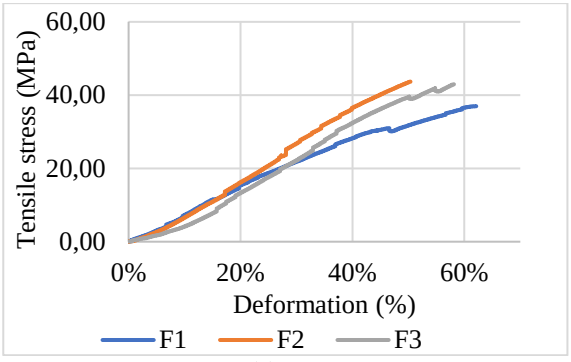

(a)

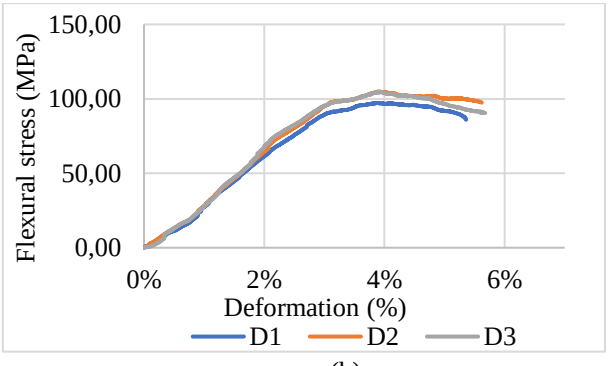

(b)

Figure 4. (a) Tensile test curve and (b) flexural test curve showing stress and deformation of samples.

2.4 Geometric deviation

For the flexural test samples, measurements were taken both before and after the annealing process to assess any impact of the treatment on the dimensions of the printed parts. The dimensions, including thickness, width, and length, were precisely measured using a caliper with a resolution of 0.01 mm and a nominal capacity of 150 mm. The changes in these dimensions were calculated, and both the average and standard deviations of these changes were recorded for analysis.

3. RESULULTS AND ANALYSIS

Figure 5 illustrates the flexural resistance of the samples, revealing a notable trend. As the printing conditions become less severe, characterized by lower temperatures for the print bed and nozzle, there is a consistent increase in resistance and elastic modulus. However, this improved resistance comes at the cost of reduced ductility in the material, which decreases under these conditions. Surprisingly, the annealing process did not appear to have a significant impact on the mechanical properties of the material in this study. It's worth noting that while annealing has been shown to alter material mechanical characteristics in previous research, its effectiveness may be hindered if the samples are exposed to moisture, as demonstrated by de Almeida et al. (2023). This could potentially explain the lack of significant changes observed in this case. This observation is further supported by the Pareto charts in Figure 6, which highlight that both nozzle and bed temperature were statistically significant factors affecting maximum resistance, ductility, and elastic modulus.

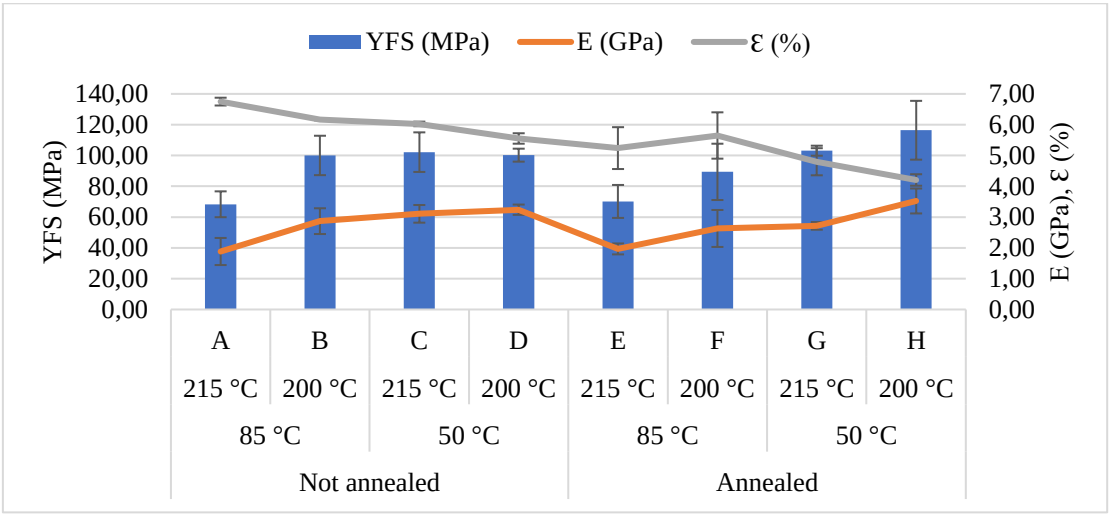

Figure 5. Maximum flexural resistance, maximum deformation, and elastic modulus of bending for all types of samples.

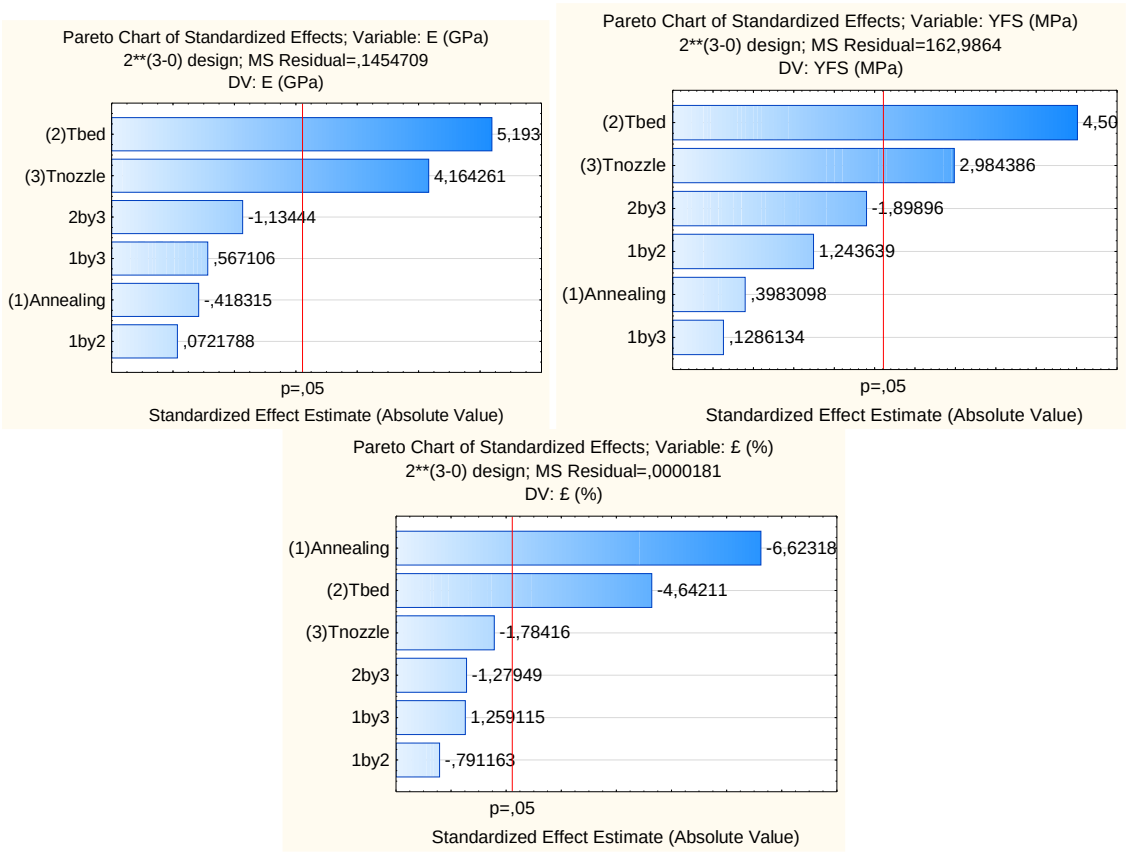

Figure 6. Pareto charts with the most influential variables for the mechanical properties evaluated in the flexural tests.

In Figure 7, the tensile resistance of the samples is depicted, and like the flexural results, there is no discernible difference observed between the annealed and printed parts in terms of maximum resistance, ductility, and elastic modulus. This observation is further supported by the Pareto chart in Figure 8, which indicates that nozzle temperature was a statistically significant factor affecting only the elastic modulus. Interestingly, the lower nozzle temperature was found to be beneficial for enhancing the material's rigidity, possibly indicating chemical changes or damage to the polymer under these more severe printing conditions.

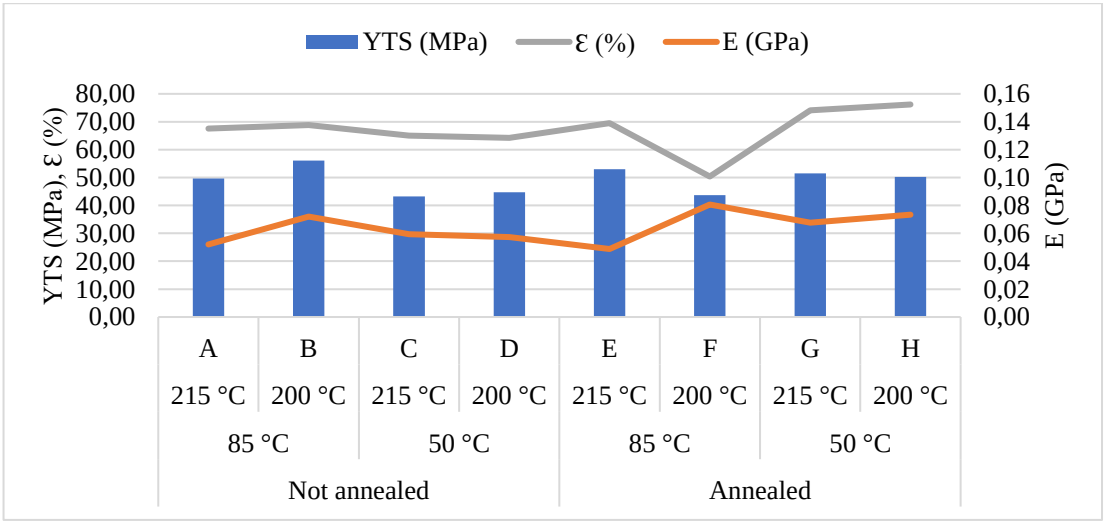

Figure 7. Maximum tensile resistance, maximum deformation and elastic modulus for all types of samples.

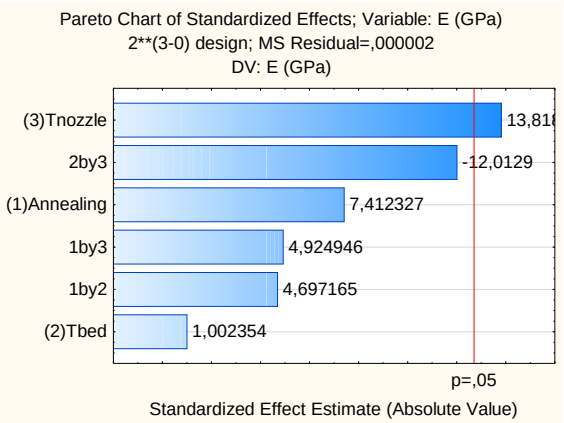

Figure 8. Pareto charts with the most influential variables for the mechanical properties evaluated in the tensile tests.

Figure 9 presents a comparison between the annealed flexural samples and the printed ones, focusing on material deformation. In all cases, an increase in thickness and a decrease in length were observed, which aligns with a common phenomenon occurring due to the crystallization process (Lluch-Cerezo et al., 2022) and the reorganization of voids (Hart et al., 2018) inherent to the printing process. Interestingly, condition B exhibited a notable increase in width, which differs from all other printing conditions. It is plausible that the combination of a lower nozzle temperature and higher bed heating in this condition resulted in fewer voids between deposited filaments. This could be attributed to improved layer adhesion and/or more consistent filament deposition, leading to the observed increase in width.

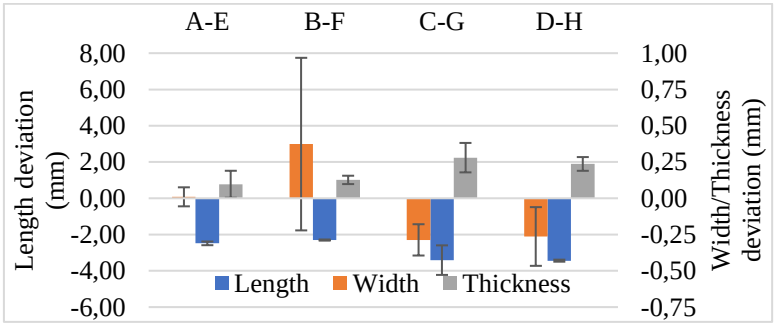

Figure 9. Dimensional change in samples due to annealing.

In Figure 10, the thermal resistance of the samples, as per ASTM D648, is depicted, demonstrating a significant increase in the maximum temperature supported by the samples when subjected to annealing. Figure 11 further reveals that bed temperature was also statistically significant, albeit at a significantly lower magnitude compared to the effect of annealing. This observed change in thermal resistance is likely attributed to the higher crystallinity of the material after annealing. Previous research (Piorkowska and Rutledge, 2013) has shown that materials with a higher proportion of crystals require more heat before melting. Additionally, when a material contains a substantial amorphous phase, this portion of the material tends to soften rapidly once the temperature exceeds the glass transition temperature (Tg), as explained by Callister (2006). Therefore, although the mechanical properties may not have exhibited significant improvements with annealing in this case, the material's heat resistance has seen a substantial enhancement. This transformation, from approximately 70°C to over 140°C, opens up a wide range of potential applications for PLA, particularly in the field of medical devices. For example, annealed parts could now be sterilized using dry air or humid vapor, typically carried out at 120°C (Vaes and Van Puyvelde, 2021).

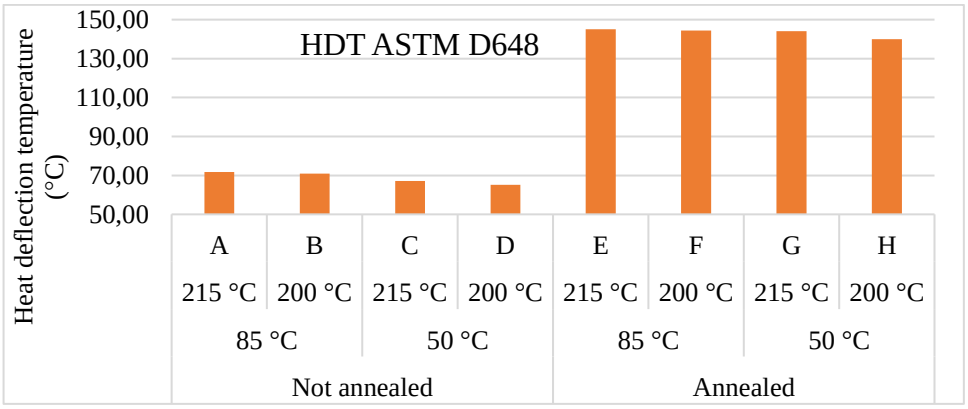

Figure 10. Heat deflection temperature measured according to ASTM D648, indicating PLA thermal resistance depending on printing conditions and annealing.

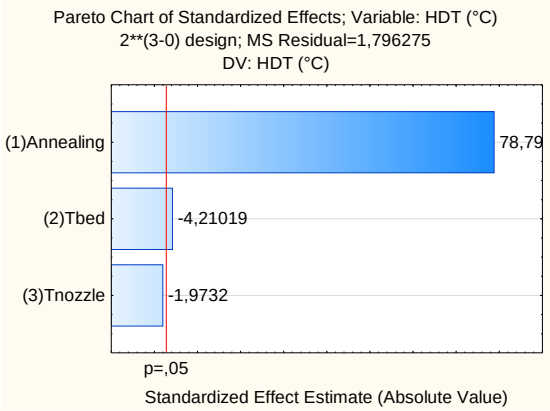

Figure 11. Pareto charts with the most influential variables for the thermal resistance of the samples.

4. CONCLUSION

This study investigated the impact of annealing on the mechanical properties and thermal resistance of PLA 3D printing samples. The research encompassed tensile tests, flexural tests, geometric deviation verifications, and a heat deflection temperature test, which serves as an indicator of material thermal resistance.

The results revealed only minor changes in material resistance due to the printing process, accompanied by slight dimensional variations. Notably, the predominant effects were attributed to printing parameters, which could potentially be linked to the material's sensitivity to humidity, contrary to what might be expected.

However, a significant improvement was observed in the thermal resistance of the polymer following the annealing process. This finding highlights an intriguing aspect of annealing for PLA, potentially expanding its applications in both industrial and consumer contexts within additive manufacturing.

5. ACKNOWLEDGEMENTS

The authors thank the CNPq, CAPES, FAPEMIG and DIRPE-UFU agencies for the financial support in the form of undergraduate and graduate scholarships.

6. REFERENCES

ASTM D638 (2014). Standard Test Method for Tensile Properties of Plastics. American Society of Testing and Materials.

ASTM D6272 (2017). Standard Test Method for Flexural Properties of Unreinforced and Reinforced Plastics and Electrical Insulating Materials by Four-Point Bending. American Society of Testing and Materials.

ASTM D648 (2018). Standard Test Method for Deflection Temperature of Plastics Under Flexural Load in the Edgewise Position. American Society of Testing and Materials.

Aliheidari, N., Tripuraneni, R., Ameli, A., Nadimpalli, S., 2017. “Fracture resistance measurement of fused deposition modeling 3D printed polymers”. Polymer Testing, 60, 94-101.

Allen, R. J., & Trask, R. S., 2015. "An experimental demonstration of effective Curved Layer Fused Filament Fabrication utilising a parallel deposition robot". Additive Manufacturing, 8, 78-87.

Bhandari, S., Lopez-Anido, R. A., & Gardner, D. J., 2019. "Enhancing the interlayer tensile strength of 3D printed short carbon fiber reinforced PETG and PLA composites via annealing". Additive Manufacturing, 30, 100922.

Callister, W. D.,2006. Fundamentos da ciência e engenharia de materiais: uma abordagem integrada. *Editora LTC. Rio de Janeiro.*

Cole, D. P., Riddick, J. C., Iftekhar Jaim, H. M., Strawhecker, K. E., & Zander, N. E., 2016." Interfacial mechanical behavior of 3D printed ABS". Journal of Applied Polymer Science, 133(30).

de Almeida, K. F., Oliveira, P. H. V., Santos, T. O., Borges, L. O., da Silva, P. A. S., Mariano, R. R. (2023). "análise dos efeitos do recozimento na resistência ao impacto de peças poliméricas impressas por FFF". In proceedings of the X11 Brazilian Congress of Manufacturing Engineering-COBEF2023, Brasília, Brazil.

Ebewele, R. O. (2000). "Polymer science and technology". CRC press.

Fernandez-Vicente, M., Calle, W., Ferrandiz, S., & Conejero, A., 2016. "Effect of infill parameters on tensile mechanical behavior in desktop 3D printing. 3D printing and additive manufacturing", 3(3), 183-192.

Hart, K. R., & Wetzel, E. D., 2018. "Fracture behavior of additively manufactured acrylonitrile butadiene styrene (ABS) materials". Engineering Fracture Mechanics, 177, 1-13.

Hoffman Tactical (2023). A Quick Look at the New Tensile Test Machine. https://www.youtube.com/watch?v=FBKQatM8QNE

Lluch-Cerezo, J., Meseguer, M. D., García-Manrique, J. A., & Benavente, R. (2022). Influence of thermal annealing temperatures on powder mould effectiveness to avoid deformations in ABS and PLA 3D-printed parts. Polymers, 14(13), 2607.

Mackay, M. E., Swain, Z. R., Banbury, C. R., Phan, D. D., & Edwards, D. A., 2017. "The performance of the hot end in a plasticating 3D printer". Journal of Rheology, 61(2), 229-236.

Matyjaszewski, K. and Möller, M., 2000. "Polymer Science: A Comprehensive Reference". Elsevier.

Percoco, G., Lavecchia, F., & Galantucci, L. M., 2012. "Compressive properties of FDM rapid prototypes treated with a low-cost chemical finishing. Research Journal of Applied Sciences, Engineering and Technology", 4(19), 3838-3842.

Piorkowska, E., & Rutledge, G. C.,2013. (Eds.). Handbook of polymer crystallization. John Wiley & Sons.

Rodríguez, J. F., Thomas, J. P., & Renaud, J. E., 2001. "Mechanical behavior of acrylonitrile butadiene styrene (ABS) fused deposition materials. Experimental investigation". Rapid Prototyping Journal.

Seppala, J. E., Han, S. H., Hillgartner, K. E., Davis, C. S., & Migler, K. B., 2017. "Weld formation during material extrusion additive manufacturing". Soft matter, 13(38), 6761-6769.

Sharafi, S., Santare, M. H., Gerdes, J., & Advani, S. G., 2021. "A review of factors that influence the fracture toughness of extrusion-based additively manufactured polymer and polymer composites". Additive Manufacturing, 101830.

Sood, A. K., Ohdar, R. K., & Mahapatra, S. S., 2010. "Parametric appraisal of mechanical property of fused deposition modelling processed parts". Materials & Design, 31(1), 287-295.

Sun, Q., Rizvi, G. M., Bellehumeur, C. T., & Gu, P., 2008. "Effect of processing conditions on the bonding quality of FDM polymer filaments". Rapid prototyping journal.

Sweeney, C. B., Lackey, B. A., Pospisil, M. J., Achee, T. C., Hicks, V. K., Moran, A. G., ... & Green, M. J., 2017. "Welding of 3D-printed carbon nanotube–polymer composites by locally induced microwave heating. Science advances, 3(6), e1700262". Butler, C. A., Mccullough, R. L., Pitchumani, R., & Gillespie Jr, J. W., 1998. An analysis of mechanisms governing fusion bonding of thermoplastic composites. Journal of Thermoplastic Composite Materials, 11(4), 338-363.

Wang, S. H., Gao, J., Lin, S. X., Zhang, P., Huang, J., & Xu, L. L., 2014, August. "Tensile deformation mechanisms of ABS/PMMA/EMA blends. In IOP Conference Series: Materials Science and Engineering" (Vol. 62, No. 1, p. 012028). IOP Publishing.

Vaes, D., & Van Puyvelde, P.,2021. Semi-crystalline feedstock for filament-based 3D printing of polymers. Progress in Polymer Science, 101411.

7. RESPONSIBILITY NOTICE

The authors are the only responsible for the printed material included in this paper.